Short Papers

Wave Propagation in Heterogeneous Anisotropic Magnetic Materials

Karine Berthou-Pichavant, Franǫise Liorzou, and Philippe Gelin

***Abstract*—In order to examine guided wave propagation in unsaturated magnetized materials, it seems reasonable to consider an alternation of layers with antiparallel magnetization in a rectangular waveguide. This approach is coherent with Schlömann's model [1] which considers partially magnetized ferrites as an alternation of antiparallel coaxial cylinders. The finite-difference time-domain (FDTD) method had been used in the case of an homogeneously filled rectangular waveguide. It is adapted here to a guide partially filled with two antiparallel magnetization layers. The modification of the FDTD algorithm at the air/ferrite and ferrite/ferrite interfaces is presented. Results are compared with the ones obtained by a mode-matching technique.**

I. Introduction

Due to their gyromagnetic properties, ferrites are being used more and more in microwave devices. This utilization requires the knowledge of the permeability tensor. Devices including ferrites are difficult to study analytically, and numerical methods such as finite-difference time-domain (FDTD) should be used. Hence, Yee's original cell [2] was modified to take magnetization into account: the discretization of the magnetic moment equation was added to Maxwell's relations, with a possibility of considering losses by Gilbert's term [3]. Totally filled rectangular waveguides have already been studied by such a method [3]–[9]. In each case, the magnetic material is saturated by applying an external field. Typical applications are the calculation of effective permeability [3], or the dispersion diagram [4]–[8]. In [8], [9], a FDTD algorithm is presented in which ferrite-frequency-dependent characteristics are introduced via inverse Fourier transform and convolution.

The long-term objective of this paper is to be able to treat components including nonsaturated ferrites. An extended FDTD method was recently presented in which the use of an empirical expression of the permeability tensor takes the partial magnetization into account [8]. The approach presented in this paper is different. Based on Schlömann's model [1], one considers partially magnetized ferrites as an alternation of thin layers, sometimes "up" magnetized (parallel to the external field), sometimes "down" magnetized (antiparallel to the external field). The problem is treated by the FDTD method in a rectangular waveguide that is only partially longitudinally filled, with two thin layers of the saturated ferrite. The algorithm is based on discretization of Maxwell and magnetic moment equations. Details about the description of the continuity equations at the air/ferrite, and up/down interfaces are presented. The results are compared with those obtained by a mode-matching method [11] in the case of scattering parameters calculations.

Manuscript received December 1, 1995; revised January 24, 1997. This work was supported by a grant from the General Council of Brittany ("La Région Bretagne").

The authors are with LEST/URA CNRS 1329, Ecole Nationale Supérieure des Télécommunications de Bretagne, 29285 Brest Cedex, France.

Publisher Item Identifier S 0018-9480(97)02906-2.

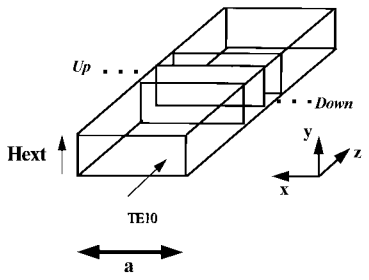

Fig. 1. "Up" and "down" layers in a rectangular waveguide.

II. Wave Propagation in Ferrites

A. FDTD Method in Saturated Ferrites

In the case of anisotropic materials [3]–[9], the FDTD method has been used to simulate wave propagation in an homogeneously filled rectangular waveguide. Thus, a number of articles have already presented ferrite FDTD discretization. In this paper, one exactly describes the expressions of the field components on different interfaces such as the ferrite/dielectric interface or the interface between two layers with an antiparallel magnetization state (Fig. 1).

Sourceless Maxwell's time-dependent curl equations are

$$rot\vec{E} = -\frac{\partial \vec{B}}{\partial t} \tag{1}$$

$$rot\vec{H} = \varepsilon_0 \varepsilon_f \frac{\partial \vec{E}}{\partial t} \tag{2}$$

where $\vec{E}$ is the electric field, $\vec{H}$ is the magnetic field, $\vec{B}$ is the magnetic induction, ε_0 is the permittivity of the vacuum, and ε_f is the dielectric constant of the ferrite. The second equation contains a scalar relation between $\vec{D}$ and $\vec{E}$, such that $\vec{D} = \varepsilon_0 \varepsilon_f \vec{E}$. The magnetic-moment equation allows one to consider the magnetic nature of the ferrite, which is magnetized here parallel to (Oy). The internal field $\vec{H}_i$ is then defined by $\vec{H}_i = H_i.\vec{a}_y$. The magnetic moment equation which includes a lossterm (Gilbert's losses) is written as

$$\frac{d\vec{M}}{dt} = -\gamma \vec{M} \wedge \vec{H} + \frac{\alpha}{Ms}\vec{M} \wedge \frac{d\vec{M}}{dt} \tag{3}$$

where $\vec{M}$ is the magnetization vector, Ms is the saturation magnetization, γ is the gyromagnetic ratio, and α is the damping term. Note that equations are written in the meter–kilogram–second–ampere (MKSA) unit system. The induction is thus given by $\vec{B} = \mu_0(\vec{H} + \vec{M})$.

Previous equations can be discretized in each homogeneous area of the guide (air or ferrite), and continuity equations must be carefully written on interfaces. In order to truncate the computational domain, second-order Engquist and Majda's absorbing boundary conditions are inserted [10]. Single-frequency excitation was used to allow the adjustment of the ABC's parameters with frequency over the whole X-band.

Excitation at the guide input then has the electric field with the following expression:

$$E_y(t, x) = 0 \quad \text{when } t < 0$$
$$E_y(t, x) = \sin\left(\frac{\pi x}{a}\right).e^{j\omega t}, \qquad \text{when } t > 0.$$

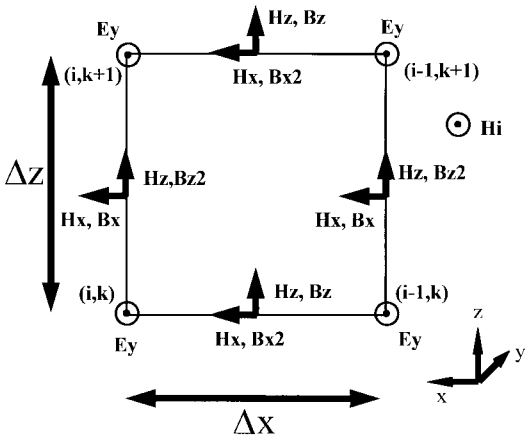

Fig. 2. 2-D extended mesh in ferrite.

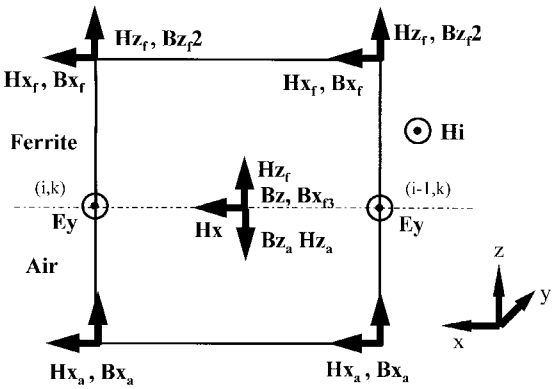

Fig. 3. Air/ferrite interface.

This allows only the TE_{10} mode to propagate. Note that the ferrite model presented here is also valid for wide-band excitation (e.g., Gaussian pulse).

The discretization of (1)–(3) which can be found in [4]–[6], is applied here for the TE_{10} mode. As a result, the three-dimensional (3-D) cell reduces to the two-dimensional (2-D) cell as shown in Fig. 2, since only Ey, Bx, Hx, Bz, and Hz components exist

$$B_x^{n+(1/2)}[i,\, k+\tfrac{1}{2}] = B_x^{n-(1/2)}[i,\, k+\tfrac{1}{2}] + \frac{\Delta t}{\Delta z}\,[E_y^n(i,\, k+1) - E_y^n(i,\, k)] \tag{4a}$$

$$B_z^{n+(1/2)}[i-\tfrac{1}{2},\, k] = B_z^{n-(1/2)}[i-\tfrac{1}{2},\, k] - \frac{\Delta t}{\Delta x}\,[E_y^n(i,\, k) - E_y^n(i-1,\, k)] \tag{4b}$$

$$E_y^n(i,\, k) = E_y^{n-1}(i,\, k) + \frac{1}{\varepsilon_0 \varepsilon_f}\left\{\frac{\Delta t}{\Delta z}[H_x^{n-(1/2)}(i,\, k+\tfrac{1}{2}) - H_x^{n-(1/2)}(i,\, k-\tfrac{1}{2})] - \frac{\Delta t}{\Delta x}[H_z^{n-(1/2)}(i+\tfrac{1}{2},\, k) - H_z^{n-(1/2)}(i-\tfrac{1}{2},\, k)]\right\} \tag{5}$$

$$H_x^{n+(1/2)} = f_0 H_x^{n-(1/2)} + f_1 B_x^{n+(1/2)} + f_2 B_x^{n-(1/2)} + f_3 B_z^{n+(1/2)} + f_4 B_z^{n-(1/2)} + f_5 H_z^{n-(1/2)} \tag{6a}$$

$$H_z^{n+(1/2)} = f_0 H_z^{n-(1/2)} + f_1 B_z^{n+(1/2)} + f_2 B_z^{n-(1/2)} - f_3 B_x^{n+(1/2)} - f_4 B_x^{n-(1/2)} - f_5 H_x^{n-(1/2)} \tag{6b}$$

Expressions for evaluating the coefficients f_i are given in [4]–[6]. Recent papers [4]–[6] outlined the necessity to calculate Hx and Hz at the same location. These components are generally evaluated by a linear interpolation on $\vec{B}$ components. For instance, B_{z2} (see Fig. 2) is evaluated by the following averaging expression:

$$B_{z2}(i,\, k+\tfrac{1}{2}) = \tfrac{1}{4}[B_z(i-\tfrac{1}{2},\, k) + B_z(i-\tfrac{1}{2},\, k+1) + B_z(i+\tfrac{1}{2},\, k) + B_z(i+\tfrac{1}{2},\, k+1)]. \tag{7}$$

The same procedure applies to the evaluation of B_{x2} (Fig. 2). Hx and Hz are then calculated with (6a) and (6b).

B. Equations on Air/Ferrite Interface

Since the accuracy of the numerical scheme near the transversal discontinuity air/ferrite is critical for FDTD, it is presented here in detail. The interface is arbitrarily located on a plane where Ey is calculated (Fig. 3). As a result, an explicit expression for this electric field tangential component can be derived by applying continuity conditions on both $\vec{E}$ and $\vec{H}$. However, Hx is not calculated on the interface. Consequently, a noncentered finite-difference is used to make Hx appear explicitly on the interface in (2).

Hence, relation (2) discretized in the air writes

$$-\varepsilon_0 \frac{Ey_a^n(i,\, k) - Ey_a^{n-1}(i,\, k)}{\Delta t} = \left[\frac{Hz_a^{n-(1/2)}(i+\tfrac{1}{2},\, k) - Hz_a^{n-(1/2)}(i-\tfrac{1}{2},\, k)}{\Delta x} - 2\frac{Hx_a^{n-(1/2)}(i,\, k) - Hx_a^{n-(1/2)}(i,\, k-\tfrac{1}{2})}{\Delta z}\right] \tag{8}$$

while in the ferrite the same equation becomes

$$-\varepsilon_0 \varepsilon_f \frac{Ey_f^n(i,\, k) - Ey_f^{n-1}(i,\, k)}{\Delta t} = \left[\frac{Hz_f^{n-(1/2)}(i+\tfrac{1}{2},\, k) - Hz_f^{n-(1/2)}(i-\tfrac{1}{2},\, k)}{\Delta x} - 2\frac{Hx_f^{n-(1/2)}(i,\, k+\tfrac{1}{2}) - Hx_f^{n-(1/2)}(i,\, k)}{\Delta z}\right]. \tag{9}$$

Then, the tangential field components continuity condition is applied [$Ey_f(i,\, k) = Ey_a(i,\, k)$, and $Hx_f(i,\, k) = Hx_a(i,\, k)$], and adding (8) and (9) yields an Ey expression on the interface at time $n\Delta t$

$$E_y^n(i,\, k) = E_y^{n-1}(i,\, k) - \frac{\Delta t}{\varepsilon_0(\varepsilon_f + 1)} \cdot \left[\frac{H_{zf}^{n-(1/2)}(i+\tfrac{1}{2},\, k) - H_{zf}^{n-(1/2)}(i-\tfrac{1}{2},\, k)}{\Delta x} + \frac{H_{za}^{n-(1/2)}(i+\tfrac{1}{2},\, k) - H_{za}^{n-(1/2)}(i-\tfrac{1}{2},\, k)}{\Delta x} - 2\frac{H_{xf}^{n-(1/2)}(i,\, k+\tfrac{1}{2}) - H_{xa}^{n-(1/2)}(i,\, k-\tfrac{1}{2})}{\Delta z}\right]. \tag{10}$$

This expression depends on Hx on each side of the air/ferrite interface and on Hz on that interface (see Fig. 3). However, since Hz is not continuous across the interface, two different subscripts are used in (10). As a result, H_{zf} is evaluated by the expression

$$H_{zf}^{n+(1/2)} = f_0 H_{zf}^{n-(1/2)} + f_1 B_{zf}^{n+(1/2)} + f_2 B_{zf}^{n-(1/2)} - f_3 B_{xf3}^{n+(1/2)} - f_4 B_{xf3}^{n-(1/2)} - f_5 H_{xf}^{n-(1/2)} \tag{11}$$

where Bx_{f3} has the following expression:

$$Bx_{f3}(i-\tfrac{1}{2},\, k) = \tfrac{1}{2}[Bx_f(i,\, k+\tfrac{1}{2}) + Bx_f(i-1,\, k+\tfrac{1}{2})]. \tag{12}$$

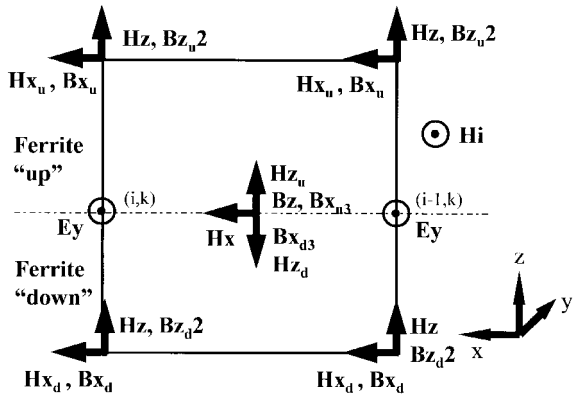

Fig. 4. "Up"/"down" interface.

H_{za} is evaluated at each time by the expression

$$H_{za}^{n+(1/2)} = \frac{1}{\mu_0} B_{za}^{n+(1/2)} \tag{13}$$

where B_{za} is given by (4b).

C. "Up"/"Down" Interface

Schlömann [1] represents the partial magnetization state by a series of coaxial cylinders, i.e., alternatively "up" or "down" magnetized. Consider this type of alternation with two antiparallel layers in the guide (Fig. 1). The "up"/"down" interface (Fig. 4) is treated exactly as the air/ferrite case. As mentioned before, the interface is located in a plane where component Ey is calculated. Index u and d represent field components in the "up" and "down" domains, respectively. Thus, according to (10), the Ey component is equal to

$$\begin{aligned} E_y^n(i,k) &= E_y^{n-1}(i,k) - \frac{\Delta t}{2\varepsilon_0 \varepsilon_f} \\ &\cdot \left[\frac{Hz_d^{n-(1/2)}(i+\frac{1}{2},k) - Hz_d^{n-(1/2)}(i-\frac{1}{2},k)}{\Delta x} \right. \\ &+ \frac{Hz_u^{n-(1/2)}(i+\frac{1}{2},k) - Hz_u^{n-(1/2)}(i-\frac{1}{2},k)}{\Delta x} \\ &\left. -2\frac{Hx_d^{n-(1/2)}(i,k+\frac{1}{2}) - Hx_u^{n-(1/2)}(i,k-\frac{1}{2})}{\Delta z} \right]. \end{aligned} \tag{14}$$

Hz_u and Hz_d are calculated by (11) and (12).

Hence, the algorithm consists of several parts. First, (4)–(6) is used with parameters corresponding to the material of each region. Then, the relation (10) and (14) derived from field continuity conditions are applied at air/ferrite and ferrite/ferrite interface, respectively.

III. Results and Comments

S-parameters are shown in Fig. 5. The reflexion coefficient and transmission coefficient magnitudes are compared with those obtained by a mode-matching technique [11]. The case of two layers having the same volume has been considered, to simulate a totally demagnetized material. One can observe that the proposed model compares reasonably well with the mode-matching technique.

The magnetization state can be modified by changing the volume of the layers. It is important to mention that the presented algorithm is also able to simulate the wave propagation in nonsaturated ferrites. In addition, it can be extended to an alternation of more layers. However, this may rapidly exhaust computing results. A possibility is to combine the proposed algorithm with the theory of periodic structures. The findings in this paper indicate that this structure will not be simple to treat with the FDTD method.

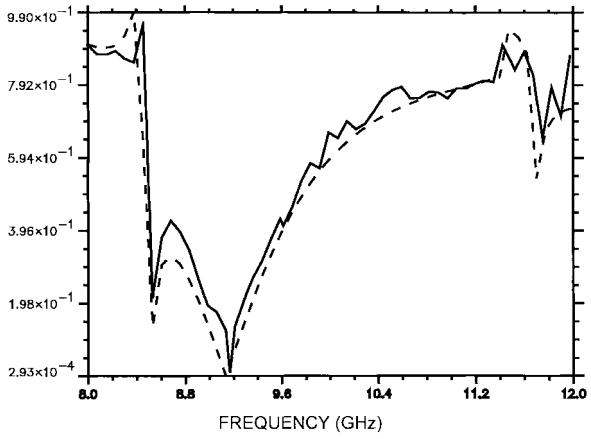

(a)

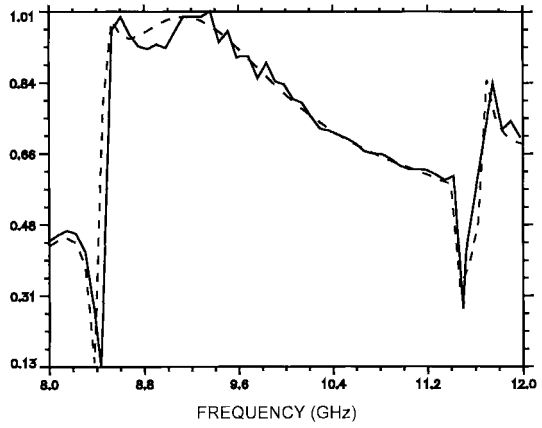

(b)

Fig. 5. (a) Module of s_{11}-parameter. "Up" domain: $Hi = 200$ Oe, $4\Pi Ms = 2000$ G, $\alpha = 0.02$. "Down" domain: $Hi = -200$ Oe, $4\Pi Ms = -2000$ G, $\alpha = 0.02$. (– – –) modal method. (—) FDTD method. $a = 22.86$ mm, $\Delta x = \Delta z = a/20$, $\Delta t = \Delta x/c\sqrt{3}$, number of time-domain iterations: 10 000, length of each layer of ferrite insertion: $5\,\Delta z$, $\varepsilon_f = 14.5$. (b) Module of s_{21}-parameter [same numerical values as in (a)].

IV. Conclusion

The FDTD method has been extended to the case of a rectangular waveguide partially filled with two antiparallel layers of a ferrimagnetic material. This study is based on discretization of Maxwell's and magnetic moment equations, and includes a careful treatment of field components on the interfaces. The results are in good agreement with those obtained by a mode-matching method. The presented algorithm constitutes an important step toward the numerical modeling of nonsaturated ferrites, considered as a juxtaposition of domains with their own magnetization.

Acknowledgment

The authors wish to thank and are indebted to Dr. M. Ney for helpful discussions and the careful reading of this paper.

REFERENCES

[1] E. F. Schlömann, "Microwave behavior of partially magnetized ferrites," *J. Appl. Phys.*, vol. 41, no. 1, Jan. 1970.

[2] K. S. Yee, "Numerical solution of initial boundary value problems involving Maxwell's equations in isotropic media," *IEEE Trans. Antennas Propagat.*, vol. AP-14, pp. 302–307, May 1966.

[3] A. Reineix, T. Monediere, and F. Jecko, "Ferrite analysis using the finite-difference time-domain (FDTD) method," *Microwave Opt. Tech. Lett.*, vol. 5, pp. 685–686, Dec. 1992.

[4] J. A. Pereda, L. A. Vielva, A. Vegas, and A. Prieto, "A treatment of magnetized ferrites using the FDTD method," *IEEE Microwave Guided Wave Lett.*, vol. 3, pp. 136–138, May 1993.

[5] ____, "FDTD analysis of magnetized ferrites: Approach based on the rotated Richtmyer difference scheme," *IEEE Microwave Guided Wave Lett.*, vol. 3, pp. 322–324, Sept. 1993.

[6] J. A. Pereda, L. A. Vielva, M. A. Solano, A. Vegas, and A. Prieto, "FDTD analysis of magnetized ferrites: Application to the calculation of dispersion characteristics of ferrites loaded waveguides," *IEEE Trans. Microwave Theory Tech.*, vol. 43, pp. 350–357, Feb. 1995.

[7] L. A. Vielva, J. A. Pereda, A. Vegas, and A. Prieto, "Calculation of scattering parameters of ferrite-loaded waveguides using the FDTD method," in *23rd European Microwave Conf.*, Madrid, Spain, Sept. 1993, pp. 285–287.

[8] J. A. Pereda, L. A. Vielva, A. Vegas, and A. Prieto, "An extended FDTD method for the treatment of partially magnetized ferrites," *IEEE Trans. Magn.*, vol. 31, pp. 1666–1669, May 1995.

[9] C. Melon, Ph. Leveque, T. Monediere, A. Reineix, and F. Jecko, "Frequency dependent finite-difference time-domain (FDTD) formulation applied to ferrite material," *Microwave Opt. Tech. Lett.*, vol. 7, no. 12, Aug. 1994.

[10] B. Engquist and A. Majda, "Absorbing boundary conditions for the numerical simulation of waves," *Math. Comput.*, vol. 31, pp. 629–651, 1977.

[11] K. Berthou-Pichavant and Ph. Gelin, "Wave propagation in non saturated ferrites: Use in modeling," in *Int. Symp. Non Linear Electromag. Syst.*, F35, Cardiff, U.K., Sept. 1995.

HBT's RF Noise Parameter Determination by Means of an Efficient Method Based on Noise Analysis of Linear Amplifier Networks

Philippe Rouquette, Daniel Gasquet, Tony Holden, and Jonathan Moult

***Abstract*— A method for the evaluation of the RF noise figure of heterojunction bipolar transistors (HBT's) is presented. The noise analysis is based on the use of the correlation matrices. The two-port device is described as an interconnection of basic two-port devices whose noise behavior is known. The circuit theory of linear noisy networks shows that any two-port device can be replaced by a noise equivalent circuit which consists of the original two-port assumed to be noiseless and possess two additional noise sources. The purpose of this paper is to obtain the four noise parameters of the device, taking into account the access resistances and inductances. The calculations presented show good agreement with measurements, and as a consequence, they permit a good estimation of the noise performance of the structure without neglecting any parasitic elements of the equivalent circuit.**

I. INTRODUCTION

Heterojunction bipolar transistors (HBT's) have recently demonstrated improved RF performances into microwave frequencies with the advent of self-aligned technologies and innovative isolation approaches to reduce parasitic effects. Therefore, it becomes important to analyze the exact causes of device limitations in terms of the HBT's equivalent circuit representation [1]–[3] and noise behavior. In Section II of this paper, the different details of the direct calculation of the HBT's T-like small signal equivalent circuit extracted from S-parameter measurements is presented. Noise analysis [4] is then presented in Section III, starting from the intrinsic impedance representation in order to calculate the noise of the total extrinsic transistor. Finally, in Section III, comparisons are presented between calculations and measurements.

II. FORMALISM FOR DIRECT EXTRACTION OF HBT'S EQUIVALENT CIRCUIT PARAMETERS

The GaInP/GaAs HBT's characterized in this work were fabricated by GEC Marconi. The authors have investigated single finger devices with effective emitter area of $3 \times 12 \ \mu m^2$ (J_1) and $3 \times 20 \ \mu m^2$ (J_2). The metal–organic chemical vapor deposition (MOCVD) grown device-layer structure consists of a 2800-Å GaAs emitter cap n^+-doped ($4 \times 10^{18}/cm^3$), two GaInP emitter layers of 200 Å n^+-doped ($2 \times 10^{18}/cm^3$) and of 1000 Å n-doped ($3 \times 10^{17}/cm^3$), 1000 Å GaAs base layer p^{++}-doped ($3 \times 10^{19}/cm^3$), 0.5-μm GaAs pre-collector n^--layer doped ($10^{16}/cm^3$) and 0.7-μm GaAs collector n^+-doped ($2 \times 10^{18}/cm^3$), all grown on a semi-insulating substrate.

The HBT's equivalent circuit used for this paper is the conventionally accepted T model [5]. This circuit is divided in three parts: the intrinsic part, the part in which the feedback capacitance is taken into account, and the extrinsic part (each of them represented by the matrix $[Z]_i$, $[Y]_j$, and $[Z]_k$), respectively. Scattering parameters have been measured for different bias points with an HP8720B network

Manuscript received March 18, 1996; revised January 24, 1997.

P. Rouquette and D. Gasquet are with the Centre d'Electronique de Montpellier, Université Montpellier II, F-34095 Montpellier cedex 05, France.

A. Holden and J. Moult are with GEC Marconi, Caswell Towcester Northands, NN 12 8EQ, U.K.

Publisher Item Identifier S 0018-9480(97)02905-0.